LANGMUIR

pubs.acs.org/Langmuir Article

Cs-RHO Goes from Worst to Best as Water Enhances Equilibrium CO_2 Adsorption via Phase Change

Le Xu, Alexander Okrut, Gregory L. Tate, Ryohji Ohnishi, Kun-Lin Wu, Dan Xie, Ambarish Kulkarni,* Takahiko Takewaki,* John R. Monnier,* and Alexander Katz*

Cite This: *Langmuir* 2021, 37, 13903−13908 Read Online

ACCESS | Metrics & More | Article Recommendations | Supporting Information

ABSTRACT: The strong affinity of water to zeolite adsorbents has made adsorption of CO_2 from humid gas mixtures such as flue gas nearly impossible under equilibrated conditions. Here, in this manuscript, we describe a unique cooperative adsorption mechanism between H_2O and Cs^+ cations on Cs-RHO zeolite, which actually facilitates the equilibrium adsorption of CO_2 under humid conditions. Our data demonstrate that, at a relative humidity of 5%, Cs-RHO adsorbs 3-fold higher amounts of CO_2 relative to dry conditions, at a temperature of 30 °C and CO_2 pressure of 1 bar. A comparative investigation of univalent cation-exchanged RHO zeolites with H^+, Li^+, Na^+, K^+, Rb^+, and Cs^+ shows an increase of equilibrium CO_2 adsorption under humid versus dry conditions to be unique to Cs-RHO. In situ powder X-ray diffraction indicates the appearance of a new phase with $Im\bar{3}m$ symmetry after H_2O saturation of Cs-RHO. A mixed-cation exchanged NaCs-RHO exhibits similar phase transitions after humid CO_2 adsorption; however, we found no evidence of cooperativity between Cs^+ and Na^+ cations in adsorption, in single-component H_2O and CO_2 adsorption. We hypothesize based on previous Rietveld refinements of CO_2 adsorption in Cs-RHO zeolite that the observed phase change is related to solvation of extra-framework Cs^+ cations by H_2O. In the case of Cs-RHO, molecular modeling results suggest that hydration of these cations favors their migration from an original D8R position to S8R sites. We posit that this movement enables a trapdoor mechanism by which CO_2 can interact with Cs^+ at S8R sites to access the α-cage.

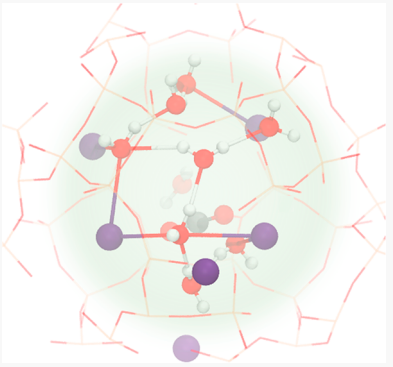

A promising approach for dealing with rising levels of CO_2 is its sequestration from flue gas.[1] Zeolites are structurally well-defined materials that adsorb CO_2 (such as zeolite LTA, RHO, CHA, KFI, MER, FAU, etc.),[2−13] while exhibiting excellent thermal, hydrothermal, and mechanical stability, high volumetric-basis CO_2 adsorption capacity, and low cost. However, an ongoing challenge with the design of zeolite adsorbents is that flue gas inevitably contains H_2O, a highly competitive adsorbate. The design of zeolites that retain significant equilibrium CO_2 adsorption capacity from humid gas mixtures remains a grand challenge,[14,15] which necessitates a deeper understanding of multicomponent CO_2 adsorption under humid conditions. The conventional belief is that humidity results in a significant decrease of the equilibrium CO_2 adsorption capacity of a zeolite, for example, demonstrated by previous studies based on both large-pore and small-pore zeolites alike and justified by the much higher heat of adsorption for H_2O compared to CO_2.[7,16,17] This has led to proposals for combating this decreased equilibrium CO_2 capacity under humid conditions by employing energy-intensive flue-gas drying.[2,7] While kinetic considerations in an actual adsorption bed unit operation can favor CO_2 over H_2O under transport control,[13,14,18] eventually, over multiple bed cycles, the adsorbed H_2O accumulates and compromises CO_2 capacity, requiring its removal.[1] If selective zeolites could be synthesized that function under equilibrated humid conditions, without compromising CO_2 capacity, this would represent a new understanding and potentially new opportunities for practical CO_2 sequestration. Here, in this manuscript, we demonstrate unique cooperativity in adsorption between H_2O and Cs^+, wherein H_2O facilitates the adsorption of CO_2 on Cs-containing RHO zeolites, leading to unprecedented higher equilibrium CO_2 adsorption capacity on Cs-RHO under humid (5% relative humidity) rather than dry conditions. In situ powder X-ray diffraction demonstrates hydration of extra-framework Cs^+ cations in Cs-RHO causes a phase change, which was previously only observed under dry conditions, at much higher CO_2 pressures of up to 4 bar.[19] Water causing such a phase change in Cs-RHO is a major discovery of this manuscript, along with insights on its repercussions for CO_2 adsorption. Ab initio molecular dynamics show this hydration moves Cs^+ cations away from positions where they would block the entrance of α-cages and supports a hypothetical trapdoor mechanism in which this

Received: September 14, 2021
Revised: September 24, 2021
Published: November 18, 2021

https://doi.org/10.1021/acs.langmuir.1c02430
Langmuir 2021, 37, 13903−13908

movement makes α-cages accessible for equilibrium CO_2 adsorption under humid conditions.

We investigated a comparative series of cation-exchanged RHO zeolite samples comprising H^+, Li^+, Na^+, K^+, Rb^+, and Cs^+ as well as a hydrothermally synthesized NaCs-RHO zeolite for CO_2 adsorption under both wet and dry conditions. Single-component CO_2 physisorption isotherms of dehydrated materials were measured at 30 °C (see Figures S2−S8, Supporting Information), as well as 80 °C for materials with significant CO_2 uptake. Among these, the material with the highest limiting single-component CO_2 uptake is Na-RHO (4.90 mmol/g at 1 bar, Figure S3, Supporting Information). Even at a low CO_2 pressure of 0.1 bar, Na-RHO adsorbs 3.65 mmol/g CO_2, which is higher than the uptakes observed at 1 bar for Li-RHO[20] and NaCs-RHO and much higher than those for Rb-RHO and Cs-RHO (see Table S1, Supporting Information). These data are consistent with the known strong interaction between Na^+ cations and CO_2 under dry conditions, which spans a variety of different framework types.[8,21]

The single-component CO_2 uptake observed for Cs-RHO is the lowest among the cation-exchanged series investigated (this uptake is only 0.46 mmol/g at 1 bar and 30 °C, which is similar to low values in the literature;[19,20] see Figure S4 and Table S1, Supporting Information). This should be contrasted with prior single-component literature data at significantly higher CO_2 pressure, which demonstrate that the Cs-RHO zeolite has the capacity to adsorb significantly higher amounts of CO_2 (about 3.4 mmol/g at 4 bar and 25 °C).[19] These higher CO_2 uptakes for Cs-RHO at pressures above 1 bar suggest that a certain fraction of space within the zeolite channels is being blocked under reduced CO_2 pressure.

We elucidate the stark differences in single-component CO_2 adsorption between Na-RHO and Cs-RHO alluded to above by considering single-component CO_2 physisorption in a mixed NaCs-RHO zeolite, which exhibits a limiting CO_2 uptake of 3.54 mmol/g at 1 bar and 30 °C in Table S1 (comparable to previous reports under similar conditions).[21] The entire single-component CO_2 physisorption isotherm at 30 °C can be described as a linear superposition of the Na-RHO and Cs-RHO data, weighted by the relative molar Na^+ and Cs^+ cation compositions of NaCs-RHO zeolite (see Figure S9, Supporting Information). Therefore, we surmise that there is a lack of cooperativity between Na^+ and Cs^+ cations in the NaCs-RHO zeolite for CO_2 adsorption.

Using thermogravimetric analysis (TGA), we compare cation-exchanged RHO zeolites for humid CO_2 adsorption by first saturating the dehydrated zeolites with H_2O at a fixed relative humidity of 5% at 30 °C, followed by conducting humid CO_2 adsorption at the same relative humidity and temperature. The first H_2O saturation experiment allows the measurement of the H_2O saturation capacity, whereas the subsequent humid CO_2 treatment at the same relative humidity (5% at 30 °C) measures the amount of CO_2 adsorption under humid conditions. Comparing results from the latter with single-component CO_2 adsorption measurements under dry conditions informs on the role of H_2O in CO_2 adsorption. In general, H_2O is expected to reduce equilibrium CO_2 uptakes due to its much higher absolute enthalpy of adsorption relative to CO_2.[16,17] Indeed, because of the latter, the presence of CO_2 is conventionally assumed not to alter equilibrium H_2O adsorption amounts at fixed relative humidity.[7,16]

All cation-exchanged RHO zeolites adsorb H_2O at 5% relative humidity and 30 °C (Figures S10−S16, Supporting Information). H-RHO, Li-RHO, and Na-RHO show similar high H_2O uptakes ranging from 9.26−9.77 mmol/g in Table S1 and Figure 1. We observe that the presence of large cations

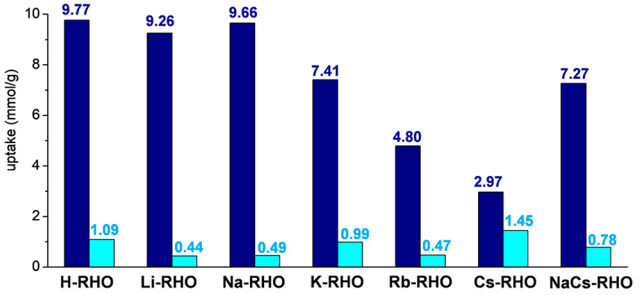

Figure 1. Equilibrium adsorption amounts of (navy blue) H_2O at 5% relative humidity relative to (light blue) CO_2 at 5% relative humidity and 1 bar on H-RHO, Li-RHO, Na-RHO, K-RHO, Rb-RHO, Cs-RHO, and NaCs-RHO zeolites. The uptakes are based on the data from multicomponent adsorption, as shown in Figures S10−S16.

such as K^+, Rb^+, and Cs^+ exchanged in RHO zeolite results in decreased H_2O uptakes of 2.97−7.41 mmol/g in Table S1 and Figure 1. The observed trends of exchange cations controlling H_2O adsorption in zeolite RHO demonstrate a decreased adsorption capacity as the row of the alkali metal cation increases, with Cs-RHO notably having the lowest H_2O uptake of 2.97 mmol/g, which is consistent with its chaotropic rather than kosmotropic nature in the Hofmeister series.[22]

Zeolite NaCs-RHO exhibits an intermediate affinity to H_2O adsorption (7.27 mmol/g H_2O), which follows a linear superposition of the pure-cation-exchanged Na-RHO and Cs-RHO data, weighted by the relative molar Na^+ and Cs^+ compositions of the NaCs-RHO zeolite (Figure S17, Supporting Information). Based on these data, as well as our data for equilibrated single-component CO_2 adsorption above, we conclude that, for both CO_2 and H_2O as pure components, Na^+ and Cs^+ cations in NaCs-RHO do not function cooperatively in causing adsorption, but rather work as independent entities, coordinating an adsorbate guest on their own separately.

Equilibrated multicomponent humid CO_2 uptakes following H_2O saturation on all zeolites, are summarized in Table S1 and Figures 1 and 2. Despite H-RHO, Li-RHO, and Na-RHO having comparable H_2O saturation capacities, the humid CO_2

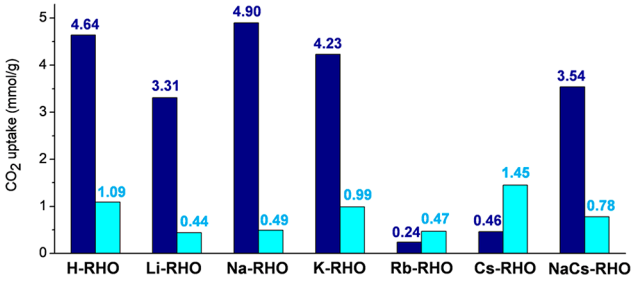

Figure 2. Equilibrium CO_2 adsorption amounts during (navy blue) single-component physisorption under dry conditions vs (light blue) multicomponent CO_2 physisorption under wet conditions (5% relative humidity) on H-RHO, Li-RHO, Na-RHO, K-RHO, Rb-RHO, Cs-RHO, and NaCs-RHO zeolites.

https://doi.org/10.1021/acs.langmuir.1c02430
Langmuir 2021, 37, 13903−13908

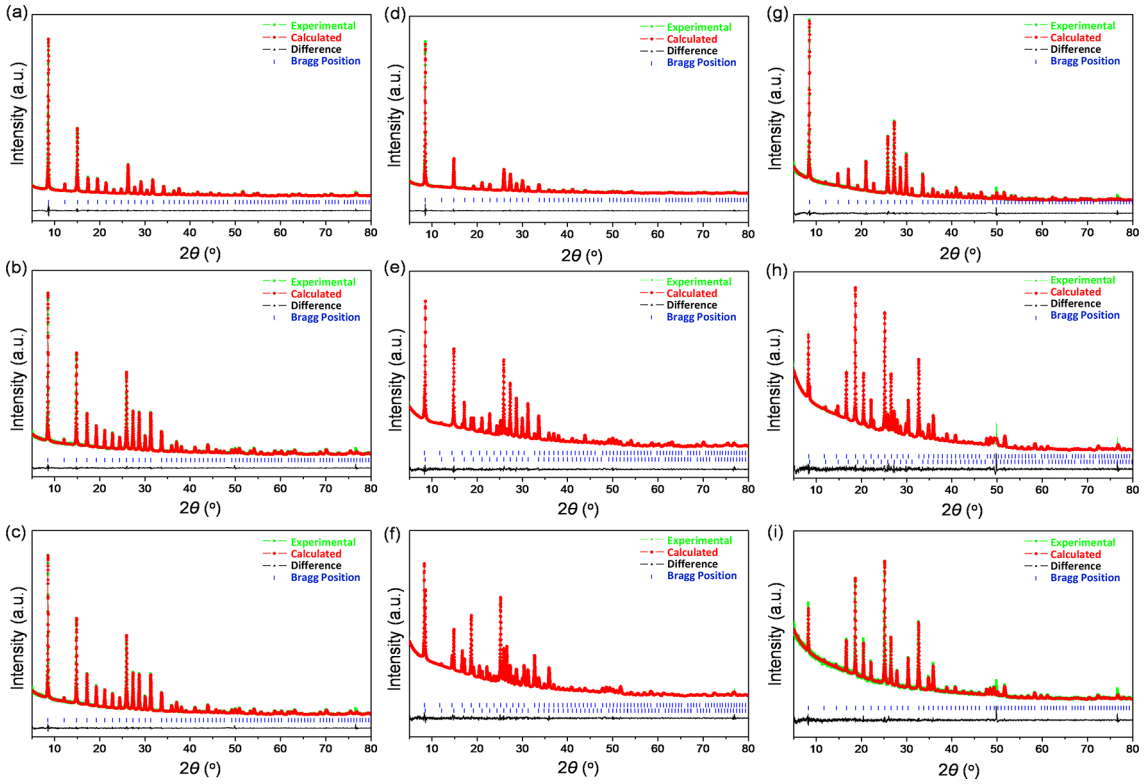

Figure 3. Profile-fitting of in situ PXRD data of (a) dehydrated Na-RHO, (b) hydrated Na-RHO at 5% relative humidity, (c) hydrated Na-RHO after CO_2 saturation at 5% relative humidity, (d) dehydrated NaCs-RHO, (e) hydrated NaCs-RHO at 5% relative humidity, (f) hydrated NaCs-RHO after CO_2 saturation at 5% relative humidity, (g) dehydrated Cs-RHO, (h) hydrated Cs-RHO at 5% relative humidity, and (i) hydrated Cs-RHO after CO_2 saturation at 5% relative humidity. The detailed crystal symmetry and unit cell parameters are summarized in Table 1.

capacities of these zeolites drop drastically as the exchange cations change from H^+ (1.09 mmol/g) to Li^+ (0.44 mmol/g) to Na^+ (0.49 mmol/g). The latter is significantly lower than the humid CO_2 uptake exhibited by NaCs-RHO of 0.78 mmol/g. We surmise that partial replacement of Na^+ by Cs^+ guest cations in RHO zeolite favors CO_2 adsorption under humid conditions.

Crucially, among all investigated materials, Cs-RHO's CO_2 capacity of 1.45 mmol/g under humid conditions is much higher than that of all other univalent cation exchanged RHO zeolites after H_2O saturation. This equilibrated CO_2 uptake on hydrated Cs-RHO is 3-fold higher relative to the value observed under dry conditions, on dehydrated Cs-RHO, of 0.46 mmol/g at the same temperature and CO_2 pressure in Figure 2. We conclude that H_2O acts cooperatively with the Cs^+ cation to facilitate CO_2 adsorption. This role of H_2O is diametrically opposed to the conventional one in the literature, of H_2O serving as a competitive adsorbent in situations involving humid CO_2 adsorption.[7,13−17,23] We surmise that this competitive adsorption of H_2O is mitigated by another role for water and the weaker interaction of H_2O with the chaotropic cations in Cs-RHO (vide supra). When comparing humid CO_2 adsorption capacities in Table S1 and Figure 2, we observe that Na-RHO, the material with the highest CO_2 uptake under dry conditions, is also the material with nearly the lowest CO_2 uptake under humid conditions. This shift is in stark contrast to Cs-RHO, which is the material with the lowest CO_2 uptake under dry conditions.

To gain further insight into the unprecedented increase in CO_2 adsorption capacity of Cs-RHO zeolite under humid compared with dry conditions, we investigated Cs-RHO, NaCs-RHO, and Na-RHO zeolites using in situ powder X-ray diffraction (PXRD), at the different stages of the TGA experiment above, corresponding to H_2O saturation followed by humid CO_2 saturation at the same relative humidity of 5%, temperature of 30 °C, and CO_2 pressure of 1 bar. The Pawley fitting of in situ PXRD data and corresponding crystal symmetry information are shown in Figure 3 and summarized in Table 1. These results demonstrate that dehydrated Na-RHO has $I\bar{4}3m$ symmetry, consistent with prior literature.[19] The symmetry of Na-RHO zeolite does not change during H_2O saturation and subsequent humid CO_2 adsorption. However, we observe an increase in the lattice parameter corresponding to $I\bar{4}3m$ symmetry after H_2O saturation, which is consistent with the expansion of the Na-RHO unit cell as a result of H_2O filling zeolite micropores. During subsequent humid CO_2 adsorption, the unit cell dimension changes only slightly, commensurate with the low amount of CO_2 adsorbed for Na-RHO zeolite under humid conditions (0.49 mmol/g, Figure 2). These results on Na-RHO are unsurprising, because the Na^+ cation is located at the S8R site[19] and, as such, can temporarily move away to allow adsorbate guests access to the α-cage, without the need for any phase change. This should be contrasted with the high amount of CO_2 adsorbed for Na-RHO under dry conditions (4.90 mmol/g, Figure 2). Under those dry conditions, the strong interaction between CO_2 and Na^+ cations promotes the movement of Na^+ via a trapdoor effect, leading to a high CO_2 uptake. Such a mechanism has been described previously on the basis of Rietveld refinement of in situ PXRD data[19,21] and involves migration of Na^+ cations away from their original S8R-site position to allow CO_2

https://doi.org/10.1021/acs.langmuir.1c02430
Langmuir 2021, 37, 13903−13908

Table 1. Crystallogaphic Information on Na-RHO, NaCs-RHO, and Cs-RHO Materials Based on In Situ PXRD in Figure 3

zeolite	in situ PXRD in Figure 3	space group and lattice parameter (phase 1)	space group and lattice parameter (phase 2)
dehydrated Na-RHO	a	$I\bar{4}3m$, 14.3421 Å	
hydrated Na-RHO	b	$I\bar{4}3m$, 14.5540 Å	
hydrated Na-RHO with CO_2	c	$I\bar{4}3m$, 14.5538 Å	
dehydrated NaCs-RHO	d	$I\bar{4}3m$, 14.5442 Å	
hydrated NaCs-RHO	e	$I\bar{4}3m$, 14.5752 Å	$Im\bar{3}m$, 14.9756 Å
hydrated NaCs-RHO with CO_2	f	$Im\bar{3}m$, 14.9761 Å	$I\bar{4}3m$, 14.5730 Å
dehydrated Cs-RHO	g	$I\bar{4}3m$, 14.5879 Å	
hydrated Cs-RHO	h	$Im\bar{3}m$, 14.9668 Å	$I\bar{4}3m$, 14.6024 Å
hydrated Cs-RHO with CO_2	i	$Im\bar{3}m$, 14.9854 Å	

molecules to access the α-cage before migrating back once the CO_2 has diffused in.

Although dehydrated NaCs-RHO has the same initial crystal symmetry ($I\bar{4}3m$) as dehydrated Na-RHO in Table 1, the symmetry of hydrated NaCs-RHO changes into a mixture of two phases after hydration at 30 °C and 5% relative humidity, as indicated by the appearance of a new phase with $Im\bar{3}m$ symmetry (Figure 3e). Furthermore, this new phase with $Im\bar{3}m$ symmetry becomes the one with the greater intensity in the in situ PXRD pattern after subsequent CO_2 adsorption (Figure 3f). The same phase transition from $I\bar{4}3m$ to $Im\bar{3}m$ has been previously reported in NaCs-RHO, upon single-component CO_2 adsorption above 200 kPa and has been used to explain high CO_2/CH_4 selectivity in this zeolite.[3]

We also observe the same phase transition from $I\bar{4}3m$ to $Im\bar{3}m$ in Cs-RHO, which, like Na-RHO and NaCs-RHO, initially exhibits $I\bar{4}3m$ symmetry in the dehydrated state, but transitions to an almost pure phase with $Im\bar{3}m$ symmetry after the first equilibrated H_2O adsorption process (the PXRD intensity of the original $I\bar{4}3m$ becomes very weak) in Figure 3h. Following the second humid CO_2 adsorption step, we observe exclusively $Im\bar{3}m$ phase in Cs-RHO zeolite in Figure 3i and Table 1.

Previously, the interaction between CO_2 and dehydrated Cs-RHO was elegantly investigated using Rietveld refinement of in situ PXRD data by Wright and co-workers.[19] Dehydrated Cs-RHO possessed $I\bar{4}3m$ symmetry, but this symmetry changed upon single-component CO_2 adsorption at 4 bar to 100% $Im\bar{3}m$ symmetry (50% change at 2 bar and 20% change at 1 bar). This prior refinement study shows that in dehydrated Cs-RHO, Cs^+ cations have two locations corresponding to the D8R and S6R sites, whereas after a single-component CO_2 adsorption at 4 bar under dry conditions, the Cs^+ cations were found to be in the same S6R sites as before CO_2 equilibration, along with a new position, corresponding to the S8R, just outside of the D8R.[21] These data suggest a mechanism to elucidate the low CO_2 uptake of dehydrated Cs-RHO at 1 bar under dry conditions (Figure S4, Supporting Information). This involves the large Cs^+ cations at the D8R sites blocking the entrance and preventing CO_2 from accessing the α-cage.[19,20] In such a mechanism, the observed phase change from $I\bar{4}3m$ to $Im\bar{3}m$ symmetry is commensurate with the opening of the D8R entrance to the α-cage, by moving Cs^+ from the D8R to S8R position. This unblocking effect would then allow a trapdoor mechanism by which CO_2 could interact with Cs^+ at S8R sites to access the α-cage, at higher CO_2 pressures (where Cs-RHO uptake of CO_2 under dry conditions increases in excess of 4 mmol/g at 9 bar, a value that is close to that described above for Na-RHO).

Based on our results in this study, we posit that H_2O solvates Cs^+ guest cations and acts as a lubricating solvation layer, which decreases the energy barrier for unblocking access to the α-cage via Cs^+ migration, according to a related trapdoor mechanism. Similar roles of solvation relating to the movement of guest cations in zeolites have been previously described[24−26] and, in particular, demonstrated for H_2O in cation-exchanged RHO zeolites.[27] Under this proposed scenario, a small amount of H_2O (corresponding to 5% relative humidity) in Cs-RHO facilitates the movement of Cs^+ cations away from their original D8R sites in the dehydrated Cs-RHO zeolite, which in turn facilitates CO_2 access. Given the relatively weak interaction of H_2O with Cs-RHO based on data in Figure 1, this small amount of H_2O is insufficient to cause competitive adsorption with CO_2 in the confines of the α-cage of the RHO zeolite, leading to a greater equilibrated CO_2 uptake for Cs-RHO under humid rather than dry conditions.

To support the hypothesis above, we have quantified the differences in the dynamics of Cs^+ cations under dry and humid conditions using ab initio molecular dynamics simulations (CP2k code, PBE functional, 10 ps production run, 1 fs time step). The zeolite composition (i.e., $Cs_{10}Al_{10}Si_{38}O_{96}$), H_2O uptake (i.e, 13 H_2O/unit cell), and unit cells (dry: $I\bar{4}3m$, wet: $Im\bar{3}m$) are consistent with the experimental samples. Figure 4a,b presents a two-dimensional histogram of the distances of the Cs^+ cations from the D8R site and the Al atoms under dry and humid conditions. Although all three high-symmetry sites are populated (Figure 4c), our AIMD calculations suggest the preferential occupation of D8R sites (66% of Cs^+ cations) under dry conditions. In contrast, the addition of H_2O (~1.3 H_2O/Cs^+ cation, similar to experiment) results in a significant Cs^+ redistribution. Specifically, while less than 10% of the Cs^+ cations occupy S8R sites under dry conditions, in the presence of H_2O, the Cs^+ cations preferentially migrate (60%) to the S8R sites. Furthermore, as evidenced by Cs^+-O_{H2O} and the Cs-D8R$_{center}$ two-dimensional distance histograms, this site redistribution arises due to the solvation of the Cs^+ cation by H_2O molecules. We observe an average Cs^+-O_{H2O} bonding distance of ~3.2 Å, in agreement with Cs^+ hydration.[28] Note that the few Cs^+ cations remaining in the D8R sites (yellow dashed oval in Figure 4d) do not interact with H_2O molecules. These AIMD simulations provide additional insights into the driving force underlying the above redistribution of cations. Specifically, the migration of Cs^+ cations from D8R to S8R sites (which are exposed to the α-cages) enables the formation of a strong hydrogen bonding network with molecular adsorbate guests in the α-cages (Figure 4e) and would be a critical step in the hypothesized trapdoor mechanism, vide supra.

In conclusion, our observations here lead to a previously unrecognized role of H_2O acting cooperatively with extra-framework Cs^+ cations to facilitate CO_2 adsorption. Our

https://doi.org/10.1021/acs.langmuir.1c02430
Langmuir 2021, 37, 13903−13908

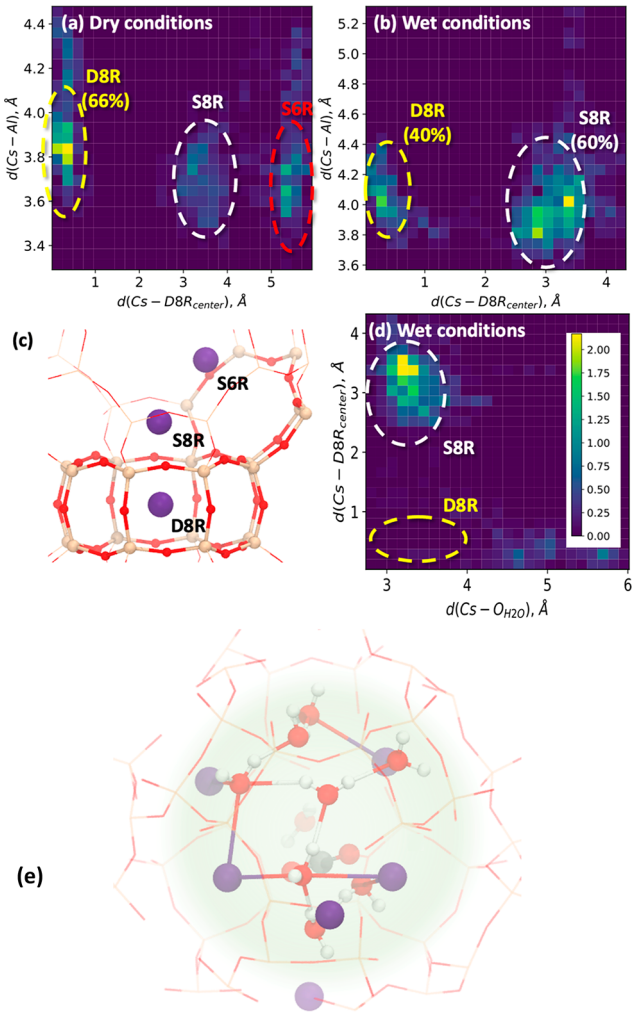

Figure 4. Two-dimensional histograms of the Cs^+ cation distances with Al atoms in (a) dry and (b) wet conditions to identify the occupancies of the (c) various high symmetry sites. (d) Two-dimensional histogram of the Cs^+ cation distances with the center of the D8R site and the oxygen atom of the H_2O molecules. (e) Representative image showing the formation of a hydrogen bonding network with the S8R Cs^+ cations and the H_2O molecules in the α-cage (green highlight). Color scheme: O (red), H (white), and Cs (purple). The RHO zeolite framework is represented using lines for better clarity.

results motivate the need to investigate CO_2 adsorption in materials under wet conditions, since these are characteristic of flue gas, including at different hydration levels.[29] We are currently in the process of proving this hypothesized mechanism by conducting a Rietveld refinement of in situ PXRD data in parallel with advanced ab initio metadynamics simulations.

■ ASSOCIATED CONTENT

Supporting Information

The Supporting Information is available free of charge at https://pubs.acs.org/doi/10.1021/acs.langmuir.1c02430.

Experimental, characterization, single-component adsorption-isotherm, and multicomponent TGA data (PDF)

■ AUTHOR INFORMATION

Corresponding Authors

Alexander Katz − *Department of Chemical and Biomolecular Engineering, University of California, Berkeley, California 94720, United States;* orcid.org/0000-0003-3487-7049; Email: askatz@berkeley.edu

Ambarish Kulkarni − *Department of Chemical Engineering, University of California−Davis, Davis, California 95616, United States;* orcid.org/0000-0001-9834-8264; Email: arkulkarni@ucdavis.edu

John R. Monnier − *Department of Chemical Engineering, University of South Carolina, Columbia, South Carolina 29208, United States;* orcid.org/0000-0003-0809-6628; Email: monnier@cec.sc.edu

Takahiko Takewaki − *Mitsubishi Chemical Corporation, Science and Innovation Center, Aoba-ku, Yokohama 227-8502, Japan*; Email: takewaki.takahiko.mb@m-chemical.co.jp

Authors

Le Xu − *Department of Chemical and Biomolecular Engineering, University of California, Berkeley, California 94720, United States*

Alexander Okrut − *Department of Chemical and Biomolecular Engineering, University of California, Berkeley, California 94720, United States*

Gregory L. Tate − *Department of Chemical Engineering, University of South Carolina, Columbia, South Carolina 29208, United States*

Ryohji Ohnishi − *Mitsubishi Chemical Corporation, Science and Innovation Center, Aoba-ku, Yokohama 227-8502, Japan*

Kun-Lin Wu − *Department of Chemical Engineering, University of California−Davis, Davis, California 95616, United States*

Dan Xie − *Chevron Energy Technology Company, Richmond, California 94801, United States;* orcid.org/0000-0003-2467-976X

Complete contact information is available at: https://pubs.acs.org/10.1021/acs.langmuir.1c02430

Notes

The authors declare the following competing financial interest(s): Coauthors Ohnishi, Takewaki, and Xie are employed by companies that may seek to commercialize aspects of CO_2 sequestration.

■ ACKNOWLEDGMENTS

The authors gratefully acknowledge funding from the CeRCaS NSF IUCRC for all characterization, and DOE, Office of Basic Energy Sciences (DE-FG02-05ER15696) for zeolite synthesis. This research used resources (Project m3820) of the National Energy Research Scientific Computing Center (NERSC), a U.S. Department of Energy Office of Science User Facility located at Lawrence Berkeley National Laboratory, operated under Contract No. DE-AC02-05CH11231.

■ REFERENCES

(1) Dewitt, S. J. A.; Awati, R.; Landa, H. O. R.; Park, J.; Kawajiri, Y.; Sholl, D. S.; Realff, M.; Lively, R. P. Analysis of Energetics and Economics of Sub-Ambient Hybrid Post-Combustion CO_2 Capture. *AIChE J.* **2021**, *67*, na DOI: 10.1002/aic.17403.

(2) Guo, X.; Wu, L.; Navrotsky, A. Thermodynamic Evidence of Flexible in H_2O and CO_2 Absorption of Transition Metal Ion Exchanged Zeolite LTA. *Phys. Chem. Chem. Phys.* **2018**, *20*, 3970−3978.
(3) Palomino, M.; Corma, A.; Jorda, J. L.; Rey, F.; Valencia, S. Zeolite Rho: A Highly Selective Adsorbent for CO_2/CH_4 Separation Induced by A Structural Phase Modification. *Chem. Commun.* **2012**, *48*, 215−217.
(4) Shang, J.; Li, G.; Singh, R.; Gu, Q.; Nairn, K. M.; Bastow, T. J.; Medhekar, N.; Doherty, C. M.; Hill, A. J.; Liu, J. Z.; Webley, P. A. Discriminative Separation of Gases by a "Molecular Trapdoor" Mechanism in Chabazite Zeolites. *J. Am. Chem. Soc.* **2012**, *134*, 19246−19253.
(5) Remy, T.; Peter, S. A.; Van Tendeloo, L.; Van der Perre, S.; Lorgouilloux, Y.; Kirschhock, C. E. A.; Baron, G. V.; Denayer, J. F. M. Adsorption and Separation of CO_2 on KFI Zeolites: Effect of Cation Type and Si/Al Ratio on Equilibrium and Kinetic Properties. *Langmuir* **2013**, *29*, 4998−5012.
(6) Georgieva, V. M.; Bruce, E. L.; Verbraeken, M. C.; Scott, A. R.; Casteel, W. J.; Brandani, S.; Wright, P. A. Triggered Gate Opening and Breathing Effects during Selective CO_2 Adsorption by Merlinoite Zeolite. *J. Am. Chem. Soc.* **2019**, *141*, 12744−12759.
(7) Li, G.; Xiao, P.; Webley, P.; Zhang, J.; Singh, R.; Marshall, M. Capture of CO_2 from High Humidity Flue Gas by Vacuum Swing Adsorption with Zeolite 13X. *Adsorption* **2008**, *14*, 415−422.
(8) Pham, T. D.; Hudson, M. R.; Brown, C. M.; Lobo, R. F. Molecular Basis for the High CO_2 Adsorption Capacity of Chabazite Zeolites. *ChemSusChem* **2014**, *7*, 3031−3038.
(9) Guo, P.; Shin, J.; Greenaway, A. G.; Min, J. G.; Su, J.; Choi, H. J.; Liu, L.; Cox, P. A.; Hong, S. B.; Wright, P. A.; Zou, X. A Zeolite Family with Expanding Structural Complexity and Embedded Isoreticular Structures. *Nature* **2015**, *524*, 74−78.
(10) Min, J. G.; Kemp, K. C.; Hong, S. B. Zeolite ZSM-25 and PST-20: Selective Carbon Dioxide Adsorbents at High Pressures. *J. Phys. Chem. C* **2017**, *121*, 3404−3409.
(11) Zhao, J.; Xie, K.; Singh, R.; Xiao, G.; Gu, Q.; Zhao, Q.; Li, G.; Xiao, P.; Webley, P. A. Li^+/ZSM-25 Zeolite as A CO_2 Capture Adsorbent with High Selectivity and Improved Adsorption Kinetics, Showing CO_2-Induced Framework Expansion. *J. Phys. Chem. C* **2018**, *122*, 18933−18941.
(12) Lozinska, M. M.; Mangano, E.; Greenaway, A. G.; Fletcher, R.; Thompson, S. P.; Murray, C. A.; Brandani, S.; Wright, P. A. Cation Control of Molecular Sieving by Flexible Li-Containing Zeolite Rho. *J. Phys. Chem. C* **2016**, *120*, 19652−19662.
(13) Ke, Q.; Sun, T.; Wei, X.; Guo, Y.; Wang, S. Enhanced Trace Carbon Dioxde Capture on Heteroatom-Substituted RHO Zeolites under Humid Conditions. *ChemSusChem* **2017**, *10*, 4207−4214.
(14) Boyd, P. G.; Chidambaram, A.; Garcia-Diez, E.; Ireland, C. P.; Daff, T. D.; Bounds, R.; Gladysiak, A.; Schouwink, P.; Moosavi, S. M.; Maroto-Valer, M. M.; Reimer, J. A.; Navarro, J. A. R.; Woo, T. K.; Garcia, S.; Stylianou, K. C.; Smit, B. Data-Driven Design of Metal-Organic Frameworks for Wet Flue Gas CO_2 Capture. *Nature* **2019**, *576*, 253−256.
(15) Datta, S. J.; Khumnoon, C.; Lee, Z. H.; Moon, W. K.; Docao, S.; Nguyen, T. H.; Hwang, I. C.; Moon, D.; Oleynikov, P.; Terasaki, O.; Yoon, K. B. CO_2 Capture from Humid Flue Gases and Humid Atmosphere Using A Microporous Coppersilicate. *Science* **2015**, *350*, 302−306.
(16) Thompson, J. A.; Zones, S. I. Binary- and Pure-Component Adsorption of CO_2, H_2O, and C_6H_{14} on SSZ-13. *Ind. Eng. Chem. Res.* **2020**, *59*, 18151−18159.
(17) Sircar, S.; Myers, A. L. Gas Separation by Zeolites. In *Handbook of Zeolite Science and Technology*; 1st ed.; Auerbach, S. M., Carrado, K. A., Dutta, P. K., Eds.; Marcel Dekker, Inc.: New York, 2013; Chapter 22.
(18) Zhou, Y.; Zhang, J.; Wang, L.; Cui, X.; Liu, X.; Wong, S. S.; An, H.; Yan, N.; Xie, J.; Yu, C.; Zhang, P.; Du, Y.; Xi, S.; Zheng, L.; Cao, X.; Wu, Y.; Wang, Y.; Wang, C.; Wen, H.; Chen, L.; Xing, H.; Wang, J. Self-Assembled Iron-Containing Mordenite Monolith for Carbon Dioxide Sieving. *Science* **2021**, *373*, 315−320.
(19) Lozinska, M. M.; Mowat, J. P. S.; Wright, P. A.; Thompson, S. P.; Jorda, J. L.; Palomino, M.; Valencia, S.; Rey, F. Cation Gating and Relocation during the Highly Selective "Trapdoor" Adsorption of CO_2 on Univalent Cation Forms of Zeolite Rho. *Chem. Mater.* **2014**, *26*, 2052−2061.
(20) Min, J. G.; Kemp, K. C.; Lee, H.; Hong, S. B. CO_2 Adsorption in the RHO Family of Embedded Isoreticular Zeolites. *J. Phys. Chem. C* **2018**, *122*, 28815−28824.
(21) Lozinska, M. M.; Mangano, E.; Mowat, J. P. S.; Shepherd, A. M.; Howe, R. F.; Thompson, S. P.; Parker, J. E.; Brandani, S.; Wright, P. A. Understanding Carbon Dioxide Adsorption on Univalent Cation Forms of the Flexible Zeolite Rho at Conditions Relevant to Carbon Capture from Flue Gases. *J. Am. Chem. Soc.* **2012**, *134*, 17628−17642.
(22) Collins, K. D.; Washabaugh, M. W. The Hofmeister Effect and the Behavior of Water at Interfaces. *Q. Rev. Biophys.* **1985**, *18*, 323−422.
(23) Li, G.; Xiao, P.; Webley, P. A.; Zhang, J.; Singh, R. Competition of CO_2/H_2O in Adsorption Based CO_2 Capture. *Energy Procedia* **2009**, *1*, 1123−1130.
(24) Li, G.; Shang, J.; Gu, Q.; Awati, R. V.; Jensen, N.; Grant, A.; Zhang, X.; Sholl, D. S.; Liu, J. Z.; Webley, P. A.; May, E. F. Temperature-Regulated Guest Admission and Release in Microporous Materials. *Nat. Commun.* **2017**, *8*, 15777.
(25) Louisfrema, W.; Paillaud, J.-L.; Porcher, F.; Perrin, E.; Onfroy, T.; Massiani, P.; Boutin, A.; Rotenberg, B. Cation Migration and Structural Deformations upon Dehydration of Nickel-Exchanged NaY Zeolite: A Combined Neutron Diffraction and Monte Carlo Study. *J. Phys. Chem. C* **2016**, *120*, 18115−18125.
(26) Porcher, F.; Paillaud, J.-L.; Gaberova, L.; Andre, G.; Casale, S.; Massiani, P. Monitoring by In Situ Neutron Diffraction of Simultaneous Dehydration and Ni^{2+} Mobility in Partially Exchanged NaY Zeolites. *New J. Chem.* **2016**, *40*, 4228−4235.
(27) Reisner, B. A.; Lee, Y.; Hanson, J. C.; Jones, G. A.; Parise, J. B.; Corbin, D. R.; Toby, B. H.; Freitag, A.; Larese, J. Z.; Kahlenberg, V. Understanding Negative Thermal Expansion and "Trap Door" Cation Relocations in Zeolite rho. *Chem. Commun.* **2000**, 2221−2222.
(28) Caralampio, D. Z.; Martinez, J. M.; Pappalardo, R. R.; Marcos, E. S. The Hydration Structure of the Heavy-Alkalines Rb+ and Cs+ through Molecular Dynamics and X-Ray Absorption Spectroscopy: Surface Clusters and Eccentricity. *Phys. Chem. Chem. Phys.* **2017**, *19*, 28993−29004.
(29) Ammouli, T.; Paillaud, J.-L.; Nouali, H.; Stephan, R.; Hanf, M.-C.; Sonnet, P.; Deroche, I. Insights into Water Adsorption in Potassium-Exchanged X-type Faujasite Zeolite: Molecular Simulation and Experiment. *J. Phys. Chem. C* **2021**, *125*, 19405−19416.

https://doi.org/10.1021/acs.langmuir.1c02430
Langmuir 2021, 37, 13903−13908